Effects of Forced Airflow Cooling on Laser Beam Heating of Volume Bragg Gratings

Sergiy Kaim*[1], Brian Anderson[1], George Venus[1], Julien Lumeau[1], Vadim Smirnov[2],
Boris Zeldovich[1], Leonid Glebov[1]

[1]CREOL, College of Optics and Photonics, University of Central Florida
[2]OptiGrate Corp., Oviedo, Florida
*Corresponding author: 4000 Central Florida Blvd, CREOL, Orlando, Florida, 32816

Abstract: Forced airflow cooling of a Volume Bragg Grating heated by a laser beam was investigated by means of simulation with COMSOL Multiphysics. In addition to air cooling of unrestricted airflow, a case of airflow directed by limiting glass plates was investigated. A number of temperature distributions and thermal deformations were obtained in simulations for different rates of airflows. Simulations proved to agree with experimental findings rather satisfactory, which makes them a good prediction tool for such type of research.

Keywords: Photo-Thermo-Refractive Glass, Volume Bragg Grating.

1. Introduction

Volume Bragg Gratings (VBG) are holographic elements recorded in Photo-Thermo-Refractive (PTR) glass. They are a relatively new invention of the last decade that has been successfully used for high power and high spectral density laser beam combining. The VBG studied in this work is one of the constituting elements of the laser beam combining system proposed and experimentally realized in [1]. In that system a set of four gratings was used to combine five laser beams with total output intensity of 750 W. Application of such high intensity beams include laser beam welding and cutting; and therefore there is a substantial engineering interest in increasing output power of such systems.

Further demand for increased output power implies necessity for higher powers of each separate laser. This in turn creates higher heat deposition in working optical elements such as VBGs, and leads to thermal deformation of PTR glass plates. These changes of shape and/or thickness of grating may cause substantial deterioration of output beam quality and even change of spectral transmission range.

In this work we consider one of the cheapest and most efficient ways of reduction of these negative effects by means of cooling the system by forced airflow. This method was recently suggested by G. Venus and demonstrated in Anderson et. al. [2]. Two situations are considered in the present work: one where VBG is cooled by unrestricted airflow, and one where VBG is cooled by an airflow directed by limiting glass plates. For each of five laser intensities we have modeled seven evenly incremented values of airflows.

2. Geometric Model of the Cooling Setup

The geometry of the 3D model used in our simulations was a reproduction of the experimental setup schematic shown on Fig 1. There a VBG has a shape of rectangular parallelepiped and is clenched in between two clamps of a metallic holder. The grating is subjected to illumination by a Gaussian laser beam propagating perpendicular to the main plain of the grating and passing through the volume of glass without altering the mechanics of the setup. The metallic holder contains a system of airways through which an external airflow is supplied to the system to withdraw heat from the surfaces of the VBG.

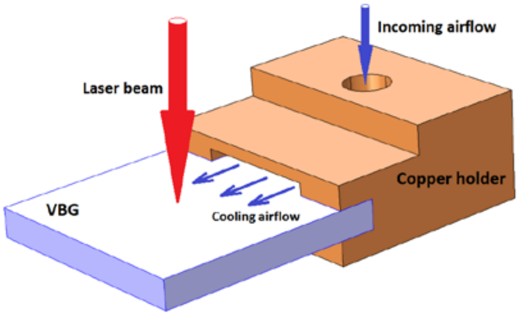

Figure 1. Schematic of the experimental setup.

Part of the system beyond the end of the grating closest to the holder is not significant for the simulation results and effectively can be left out of the model to provide for simulations that are more efficient and consume less computational resources. Fig. 2 shows the actual COMSOL geometry used in our simulations. There the airways were essentially substituted with two airflow inlets on the border adjacent to the grating, and the whole glass plate of grating together with metallic holder submerged into an air box. Table 1 contains main dimensions of the setup.

Table 1: Main dimensions of system with unrestricted VBG

Grating	$2.74\cdot10^{-3}$ x $2.2\cdot10^{-2}$ x $2.2\cdot10^{-2}$	m
Metallic Holder	$2.275\cdot10^{-3}$ x $3.5\cdot10^{-3}$ x $2.2\cdot10^{-2}$	m
Air Inlet (x2)	$1.135\cdot10^{-3}$ x $1.2\cdot10^{-2}$	m
Air Box	$1.507\cdot10^{-2}$ x $2.748\cdot10^{-2}$ x $3.304\cdot10^{-2}$	m

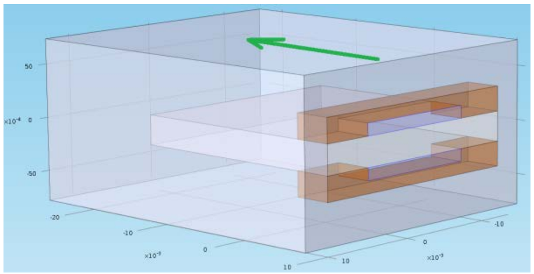

Figure 2. Geometry of VBG used for COMSOL simulations. The arrow points in the general direction of airflow.

The alternative case of the system limited by two glass plates has very similar geometry. The main difference was that two glass plates in shape of rectangular parallelepipeds are now being "glued" to the top and bottom sides of the metallic holder. The system is still submerged into an air box but the top and bottom borders of this box are now adjacent to borders of the limiting glass plates (Fig. 3). Geometrical dimensions of the limiting glass plates and the air box for this alternate case are shown in Table 2.

Table 2: Dimensions of limiting glass plates and the corresponding air box

Limiting Glass Plates	$1.85\cdot10^{-3}$ x $2.2\cdot10^{-2}$ x $2.2\cdot10^{-2}$	m
Air Box	$2.2\cdot10^{-2}$ x$3.304\cdot10^{-2}$ x $1.098\cdot10^{-2}$	m

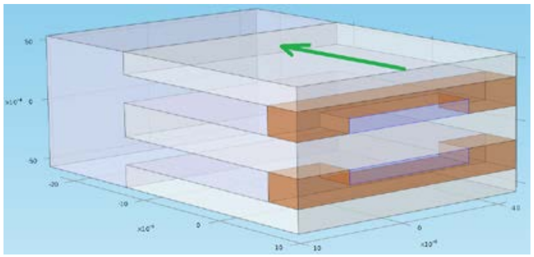

Figure 3. Geometry of VBG limited by glass plates used for COMSOL simulations. The arrow points in the general direction of airflow.

3. Thermal Model

PTR glass is a novel material not widely known outside of specialized research groups and companies working with it. Therefore, to complete our model with corresponding material characteristics we used both COMSOL materials library and created our own material to use parameters specific for PTR glass only. Air was chosen for the volume of air box, metallic holder was made out of copper, and the VBG was chosen to be made of our newly created material with parameters outlined in Table 3.

Table 3: Material characteristics of Photo-Thermo-Refractive glass

Coefficient of Thermal Expansion	$9.5\cdot10^{-6}$	1/K
Heat Capacity at Constant Pressure	840	J/(kg*K)
Density	2500	kg/(m^3)
Thermal Conductivity	1.05	W/(m*K)
Young's Modulus	$6.4\cdot10^{10}$	Pa
Poisson Ratio	0.2	dimensionless
Refractive Index	1.4891	dimensionless

To study different heat transfer mechanisms, the “Thermal Stress” interface from module “Structural Mechanics” was chosen. In this interface 10 models were chosen to describe initial conditions and evolution of the system. “Thermal Linear Elastic” model was chosen for domains containing VBG and copper holder. Boundary conditions were chosen by the “Free” model for all boundaries except the boundaries of the copper holder adjacent to the air box. For those adjacent boundaries a “Fixed Constraint” model was chosen to effectively reproduce rigid connection of the holder to its extension which exists in experimental setup but which is left out of the current modeling situation. Heating of the VBG with laser beam was taken into account by introducing model “Heat Source” for domains of VBG and of copper holder. The model “Heat Transfer of Fluids” was responsible for transfer of heat from surfaces of the VBG and the holder. The border of the air box furthest away from the inlet of airflow is assumed to take in all the excessive heated air coming in into the system during forced air cooling. Thus a model “Outflow” is applied to that border. To imitate the absorption of any extra heat in the system far away from the borders of the heated surfaces we set boundaries of our air box to a constant ambient temperature by applying a model “Temperature”.

An identical set of conditions was applied for the alternate case of airflow being directed by a couple of limiting glass plates and domains containing glass plates were effectively treated the same way as the domain containing the VBG. Plates had a condition of rigid connection on the borders adjacent to the copper holder. The only parametric difference (due to experimental properties of material of glass plates) is that absorption coefficient of glass plate was 140 times smaller than that of the VBG.

Heating of the grating was simulated to have 2D Gaussian distribution with the center of the beam matching the geometrical center of the grating. The complete expression used had a form

$$Q_{in}(x,y,z) = P_0 \cdot \alpha \cdot \frac{1}{\pi \cdot \sigma_x \cdot \sigma_y} \cdot \exp\left(-\frac{(x-x_0)^2}{2 \cdot {\sigma_x}^2} - \frac{(y-y_0)^2}{2 \cdot {\sigma_y}^2}\right) \cdot \exp(-\alpha \cdot |z|), \qquad (1)$$

where P_0 is total power of laser; α is absorption coefficient of PTR glass; σ_x and σ_y are standard deviations of the beam controlling its width in in x and y directions, correspondingly; x_0 and y_0 are coordinates of the center of the beam. Here parameter P_0 can be set up to the appropriate value of total power to model lasers with corresponding power values. Parameter α is a constant value for PTR glass and was taken to be $2.3 \cdot 10^{-2}$ m^{-1}. The heating beam was symmetrical with diameter of $6 \cdot 10^{-3}$ m (FWe^{-2}IM). Normalization of Gaussian is provided by the coefficient in front of the exponent. The first exponent itself defines the shape of the Gaussian beam and the second one is responsible for decrease of heat deposition in glass as beam propagates deeper through volume of glass.

To implement this distribution in our simulations a model “Analytic” was created within interface “Global Definitions”. That model contained the first exponent of the Gaussian and was effectively setting up its shape. To add normalization condition and specific parameters of the beam a separate variable was created in the “Definitions” of interface “Model”. This variable had all the constants defined in (1) along with reference to the newly created analytic function.

4. Fluid Dynamics Model

Simulation of the cooling airflow and accounting for heat carried away by this flow from the surfaces of the system was possible due to use of the interface “Turbulent Flow, k-ε” from module “Fluid Flow”. Models “Fluid Properties” and “Initial Values” are the default models included; they specified properties of air and initial velocities, correspondingly. Air pressure was taken to be normal atmospheric pressure and the initial temperature was set to 20°C. The default model “Wall” applied to all surfaces of the grating and metallic holder submerged into the air box. An air influx and control of its initial velocity is performed within a model “Inlet”. This model was applied to the surface area in the place where air shafts meet the border of the air box. Influx velocity vector was set in perpendicular to the plane of the inlets, which in turn, is parallel to the main plain of the VBG. The excess of air created by this additional influx is taken away from the simulated system by application of a model "Outlet" to the border located farthest away from the VBG. A "Symmetry" model is implemented to all the remaining borders of the air box.

Yet again, for the case of the VBG limited by glass plates, the domains of these plates were subjected to the same conditions as the domain containing the VBG.

One of the most important decisions defining precision and time of computations in these simulations was choice of the meshing. Study of effects of forced air cooling requires attention to the phenomena of heat exchange between solid surfaces of the system and air flux along those surfaces. Thus for better understanding of those phenomena and to provide for more precise simulations we applied an option "Boundary layers" to all boundaries in the domain of the air box. Number of boundary layers was taken to be 25 with stretching factor of 1.2. Setting thickness of first layer manually allows for better control of calculation precision. It was set to the absolute value of $0.7 \cdot 10^{-4}$ m, and its relative value compared to the length of the VBG was 0.025. In all other domains of the system we applied the option "Free Tetrahedral" with maximum element size set up manually to $0.9 \cdot 10^{-3}$ m.

Calculation times were ranging from 3.5 hours for small influx velocities (IBM PC computer with Intel Core 2 Quad processor, 2.66 GHz, 8GB memory) and over 4 hours as velocities were approaching closer to their maximum values.

5. Comparison of Simulation and Experimental Results

For the purposes of this research, the most important goals were obtaining simulated temperature distributions in the volume of glass, obtaining deformations of the VBG caused by thermal effects, comparison of simulated results to experimental ones, and comparison of simulated results between the cases of unlimited VBG and VBG limited by glass plates.

For a case of unlimited VBG we modeled four laser beam powers with each of them corresponding to experimental ones. Namely, power values of 4.5kW, 6.7kW, 8.9kW and 11kW were modeled. In case of VBG restricted by glass plates the power values of 4.5kW, 6.1kW, 6.7kW, 8.9kW and 11kW were chosen. For each of the laser beam power we conducted simulations with the following cooling airflows (in m/s) 0.0, 17.3, 34.6, 51.9, 69.1, 86.4, 103.7, 121.

An example of distribution of surface temperature increases and corresponding thermal deformations of VBG for laser power of 11kW and airflow of 86.4 m/s is shown on Fig. 4(a) for unrestricted VBG, and on Fig. 4(b) for restricted VBG.

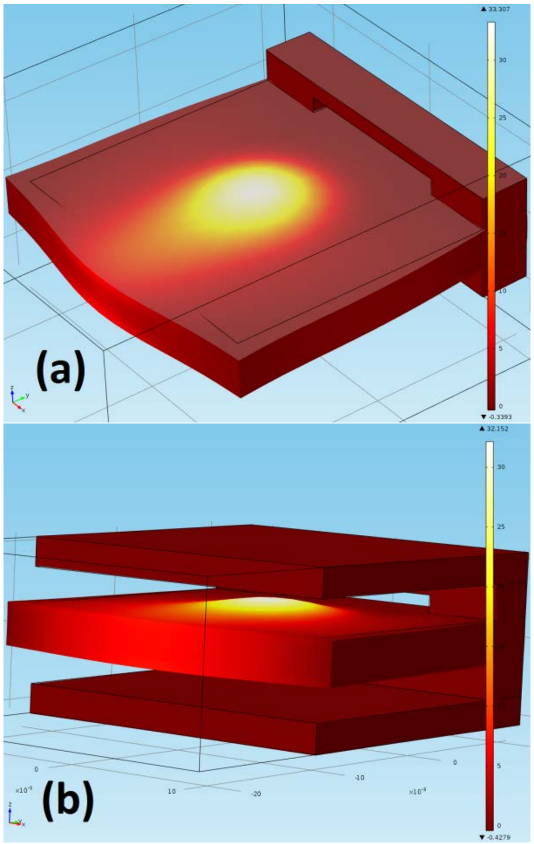

Figure 4. Increase of temperatures (as compared to the ambient one) for: (a) the unrestricted VBG. (b) restricted VBG. In both cases laser power and airflow velocity were 11kW and 86.4 m/s, respectively.

For illustration purposes, deformation amplitudes are increased by approximately 2000 times. By choosing option "Cut Line 3D" in the interface "Data Sets" we created four line probes in the tested VBG. Two probes were put on the surface of the grating. Both of them go through the center of the grating but one is parallel to the direction of airflow, and the other one is perpendicular to it. Other two probes were running though the volume of the VBG, midway between the surfaces. Similarly, both probes were going through geometrical center of the grating: one probe in parallel to direction of an airflow, and the other one in perpendicular to it. Graphs of temperatures along these line probes for the above example of unrestricted VBG of 11kW and airflow of 86.4 m/s are shown on Fig. 5.

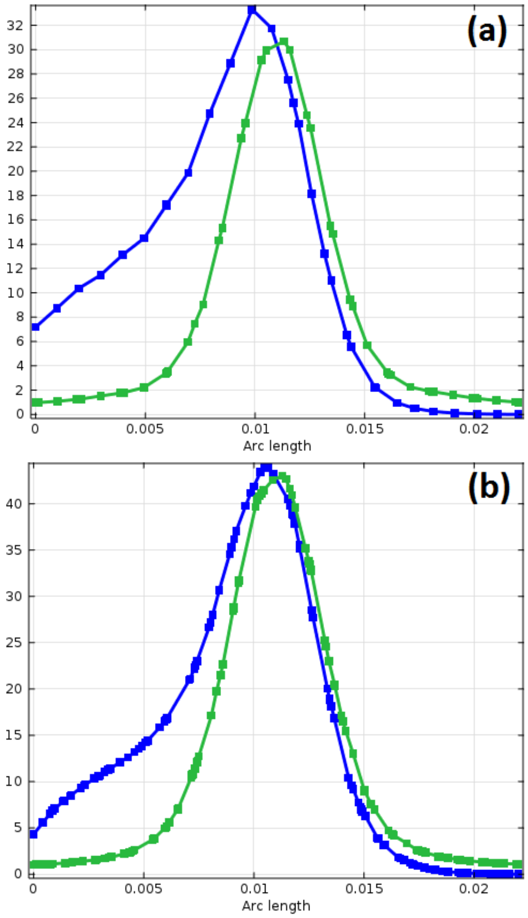

Figure 5. (a) Surface temperature increase (compared to the ambient temperature) for unrestricted grating; (b) Temperature increase inside of the grating. Blue lines correspond to probes parallel to direction of airflow, green lines correspond to perpendicular direction. In both cases laser power and airflow velocity were 11kW and 86.4 m/s, respectively.

The experiment conducted for the same systems allowed only a limited number of characteristics to be measured. Among those relevant to our simulations were peak temperatures inside of VBG for different airflows. Fig. 6 shows comparison of peak temperature increases as compared to ambient temperature measured along the probes inside VBG and those measured experimentally for a case of grating not restricted by glass plates. For a case of limited VBG there was conducted experiment only for one laser power of 6.1kW. Comparison of its results with our simulation is shown on Fig. 7.

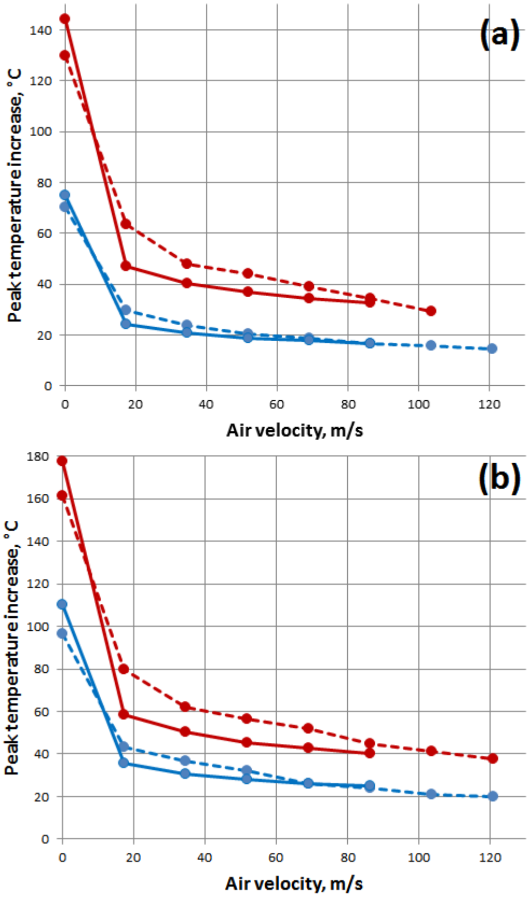

Figure 6. Peak temperature increase compared to the ambient temperature of the system for unrestricted VBG. In all cases, solid and dashed lines are for simulated and experimental data, respectively. (a) Blue curves correspond to laser power of 4.5kW and red curves correspond to laser power of 8.9kW; (b) Blue curves correspond to laser power of 6.7kW and red curves correspond to laser power of 11kW.

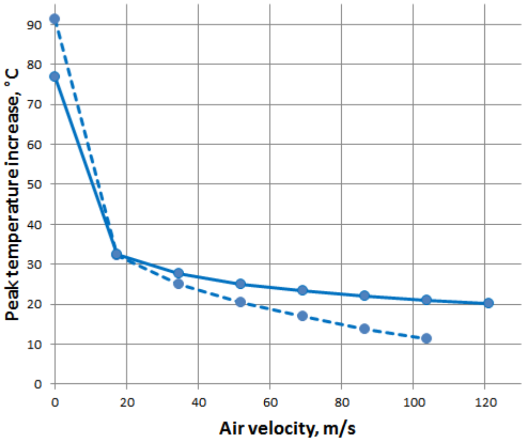

Figure 7. Peak temperature increase compared to the ambient temperature of the system for restricted VBG at laser power of 6.1kW. Solid and dashed lines are for simulated and experimental data, respectively.

Overall discrepancy between simulated and experimental data temperatures was around 15%, with the maximum reaching 27% for some combinations of laser power and rate of airflow. Fig. 8 shows comparison of two experimental data sets for unrestricted and restricted VBGs for a case of laser powers of 6.7kW and 6.1kW. It is apparent from the graph that all the temperatures for a VBG limited by a pair of glass plates are clearly lower than those of an unrestricted VBG at the same rates of airflows.

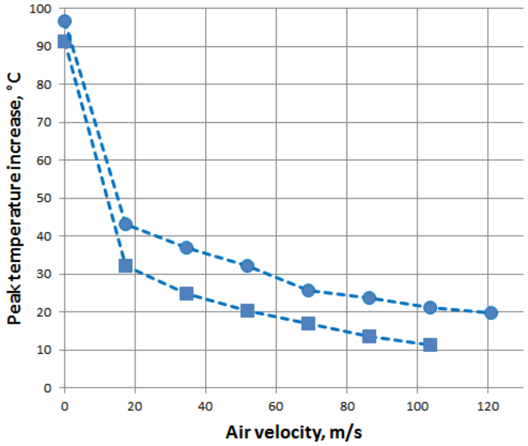

Figure 8. Experimental data on peak temperature increase (compared to the ambient temperature). Dots correspond to the system for unrestricted VBG at laser power of 6.7kW while squares correspond to the VBG limited by glass plates at laser power of 6.1kW.

Unfortunately, due to experimental limitations there is no data about peak temperatures of limited VBG for any other powers of laser beams. But as we saw above COMSOL simulation data describes experimental temperatures of both systems with sufficient precision. There comparison of the curves obtained by simulations for cases of both unrestricted and restricted VBGs must be a good predictor of an experimental situation. Indeed, overlaying curves corresponding to the same laser powers for both cases shows a slight trend of the cooling process to be more efficient in case of a VBG limited by glass plates (Fig. 9). It is more obvious for small initial velocities of cooling airflow and this discrepancy rather quickly diminishes as rate of airflow increases.

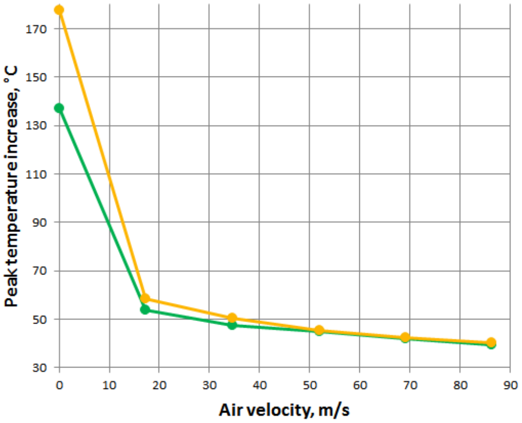

Figure 9. Simulation results on peak temperature increase (compared to the ambient temperature) for laser power of 11kW. Yellow curve corresponds to unrestricted VBG and green curve to a VBG limited by glass plates.

6. Conclusions

Thus we have shown via COMSOL modeling and physical experiment that forced air cooling of VBG is an inexpensive and efficient way of substantially reducing negative effects of thermal deformation of PTR glass and this effect is being enhanced in case of limiting a VBG by a pair of glass plates.

7. References

1. D. Drachenberg, I. Divliansky, V. Smirnov, G. Venus, and L. Glebov, "High Power Spectral Beam Combining of Fiber Lasers with

Ultra High Spectral Density by Thermal Tuning of Volume Bragg Gratings.” Proc. of SPIE vol. 7914 (2011).

2. Brian Anderson, Sergiy Kaim, George Venus, Imtiaz Majid, Julien Lumeau, Vadim Smirnov, Boris Zeldovich, Leonid Glebov. “Forced Air Cooling of Volume Bragg Gratings for Spectral Beam Combination.” Proceedings of SPIE 8601, Fiber Lasers X: Technology, Systems, and Applications (March 2013).